Journal of Biomolecular NMR, **11:** 437–444, 1998.
KLUWER/ESCOM

Efficient multiple-solvent suppression for the study of the interactions of organic solvents with biomolecules

Claudio Dalvit
Novartis Pharma AG, CH-4002 Basel, Switzerland

Received 4 November 1997; Accepted 9 January 1998

Key words: excitation sculpting, hydration, multiple-solvents suppression, organic solvents, pulsed field gradients

Abstract

A modification of the excitation sculpting sequence [Hwang, T.-L. and Shaka, A.J. (1995) *J. Magn. Reson.*, **A112**, 275–279] for achieving efficient multiple-solvents suppression in 1D and 2D ^{1}H NMR experiments is presented. Implementation of this scheme in the ePHOGSY experiment allows rapid and sensitive detection of weak interactions between organic solvents or small molecules and biomolecules. Application of the techniques to the peptide Sandostatin® dissolved in H_2O and DMSO is demonstrated.

The study of the interaction of organic solvents and small molecules with proteins and other biomolecules by NMR has recently gained some interest (Liepinsh and Otting, 1997; Ponstingl and Otting, 1997). The identification of the binding sites on the surface and/or interior of a protein may provide valuable information for rational drug design. For example, in SAR by NMR (Shuker et al., 1996) structural information on small molecules, binding weakly on different sites of the protein, is used to guide the design of chemical linkers between these ligands. The tethered molecule can then result in a high-affinity compound.

Several H_2O selective one-dimensional and two-dimensional experiments have been proposed in the literature for studying the interactions between H_2O and biological macromolecules (Otting and Wüthrich, 1989; Clore et al., 1990; Otting et al., 1991; Moonen et al., 1992; Grzesiek and Bax, 1993a; Kriwacki et al., 1993; Mori et al., 1994; Otting and Liepinsh, 1995; Birlirakis et al., 1996; Böckmann and Guittet, 1996; Mori et al., 1996; Wider et al., 1996; Hwang et al., 1997). A member of this family of experiments is the ePHOGSY (Dalvit and Hommel, 1995; Dalvit, 1996), which results in high sensitivity spectra devoid of artefacts. This class of experiments in principle can also be applied to the studies of organic solvents, small molecules with proteins. However, their application in these studies requires excellent multiple-solvent suppression. Often only extremely weak interactions are observed between the solute and the solvents. Therefore these effects will not be visible if the suppression of the solvent signals is not perfect.

We propose here a modification of the 1D and 2D ePHOGSY pulse sequences which results in remarkable multiple-solvent suppression without resorting to the deleterious presaturation schemes. The method for achieving efficient multiple-solvent suppression is a simple modification of the excitation sculpting sequence (Hwang and Shaka, 1995) proposed recently. The soft 180deg pulse of the original version is replaced here with a frequency shifted laminar pulse (SLP) (Patt, 1992) with excitation at different frequencies. The scheme is:

$$(\frac{\pi}{2}) - \mathrm{G1} - (\pi)^{\mathrm{SLP}}_{\mathrm{soft}} - (\pi) - \mathrm{G1} - \mathrm{G2} - (\pi)^{\mathrm{SLP}}_{\mathrm{soft}} - (\pi) - \mathrm{G2} \quad (1)$$

where G1 and G2 are gradients of different strength. The $(\pi)^{\mathrm{SLP}}_{\mathrm{soft}}$ pulses contain as many modulations as the number of solvent signals to be suppressed. This soft π pulse is either a selective rectangular pulse or a strongly truncated Gaussian pulse (Bauer et al., 1984). For better performance an entire EXORCYCLE (Bodenhausen et al., 1977) is applied at one or both elements comprising the scheme, resulting in a 4 or 16 step phase cycle, respectively. If necessary, a short spin-lock period can also be inserted in se-

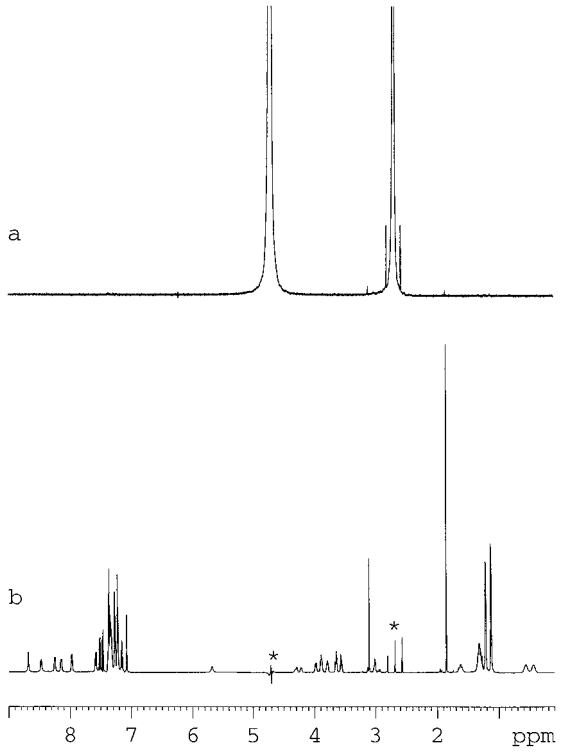

Figure 1. (a) One-dimensional reference spectrum recorded for a 4 mM solution of Sandostatin, pH 7.6 in 250 μl H_2O, 250 μl DMSO (50 μl D_2O) at 297 K. (b) One-dimensional spectrum recorded with scheme (1) (see text). The phases for the four 180° pulses in (1) are from left to right 1st: 4(−x), 4(−y), 4(x), 4(y), 2nd: 4(x), 4(y), 4(−x), 4(−y), 3rd: −x, −y, x, y, 4th: x, y, −x, −y. The phase of the receiver is: 2(x, −x), 2(−x, x). A total of 16 scans were acquired for (b). Excellent spectra could be achieved also with only four scans. The length of the soft 180° frequency shifted laminar pulse was 2.9 ms and the repetition time was 2.5 s. The length of the sine-shaped gradients was 1 ms and the gradient recovery delay was 200 μs long. The strength of the gradients along the three axes x, y, z was 4.5, 4.6, 6.7 G/cm for G1 and 12.1, 12.3, 16.4 G/cm for G2. The asterisks in (b) indicate the residual solvent signals.

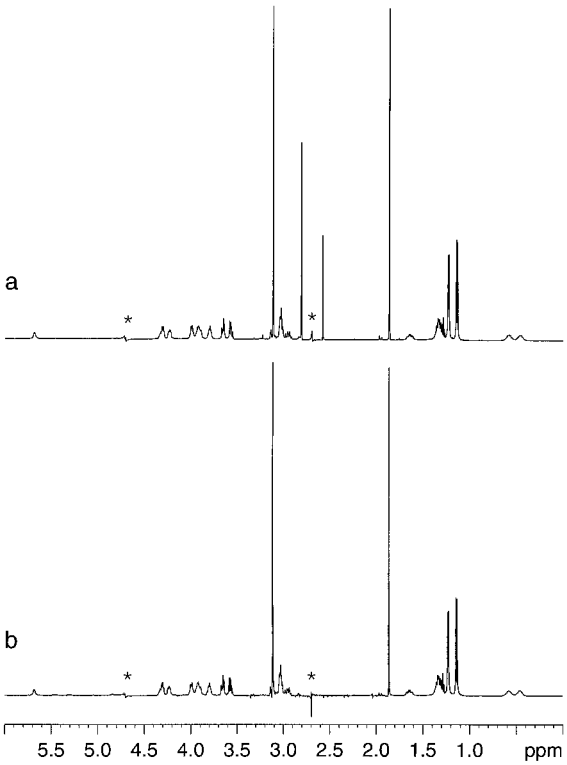

Figure 2. (a) Spectrum obtained with scheme (1); and (b) spectrum obtained with scheme (1) and a ^{13}C filter. The sample is a 2 mM solution of Sandostatin in 50% H_2O and 50% DMSO. In (b) the length of the sine-shaped gradients was 1.2 ms and the gradient recovery time was 300 μs long. The asterisks indicate the residual solvent signals. Other parameters are the same as in Figure 1. Note that signals located at 0.2 ppm from the solvent frequencies are easily detected and only partially attenuated.

quence (1) before the acquisition period in order to destroy the small amount of homonuclear antiphase magnetization created during the scheme.

The system chosen to test the performance of these experiments is a 4 mM sample of the peptide Sandostatin® (D-Phe-Cys-Phe-D-Trp-Lys-Thr-Cys-Thr(Ol)) dissolved in 250 μl H_2O, 250 μl h_6-DMSO and 50 μl D_2O. This corresponds to a concentration of 25.25 M (50.5 M in protons) for H_2O and of 5.83 M (34.98 M in protons) for DMSO. For the experiments of Figure 2 the sample concentration was 2 mM. All experiments have been recorded with a 600 MHz spectrometer comprising a Bruker actively shielded magnet and an Avance Bruker console. The gradients were generated with an ACCUSTAR™ unit connected to a 5 mm triple-resonance inverse probe equipped with actively shielded x, y, z-gradient coils. The maximum strength of 100% corresponds to gradients of 44.9, 45.6 and 60.7 G/cm for the x, y and z directions, respectively.

Figure 1a shows the one-dimensional reference spectrum of the peptide where the only observable resonances are those of the two solvents and of the ^{13}C satellite signals of DMSO. Figure 1b shows the spectrum obtained with the excitation sculpting sequence of scheme (1) where the $(\pi)^{SLP}_{soft}$ pulse is a frequency shifted laminar 180° soft pulse with selective excitation at the two solvent frequencies. Optimization of the experiment is carried out in an interactive way. The difference in chemical shift between the two solvents extracted from Figure 1a is used for the creation of the SLP. It is then increased until a minimum solvent

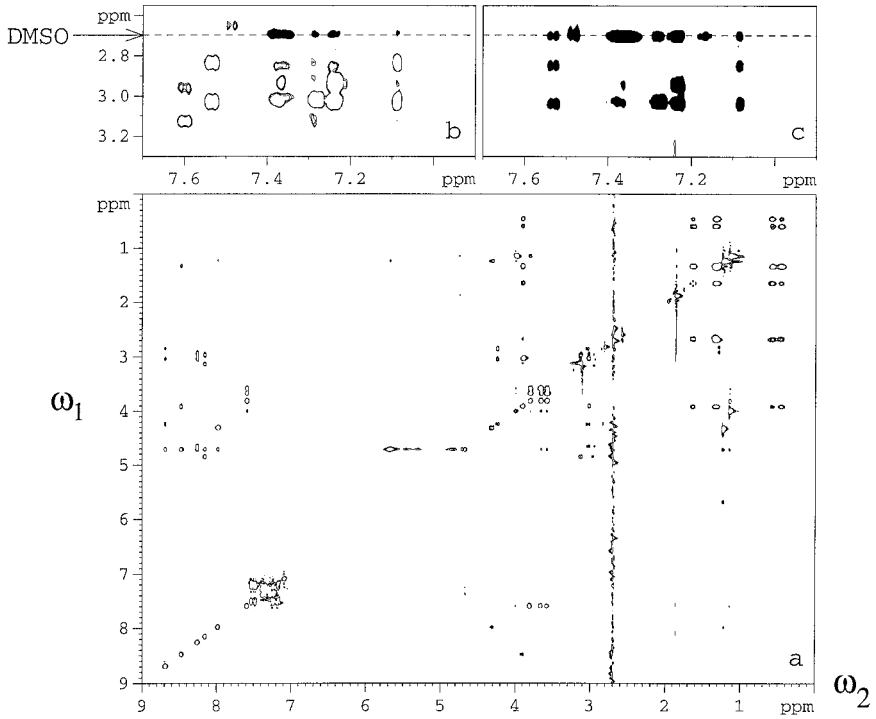

Figure 3. (a) 2D TOCSY spectrum recorded with multiple-solvent suppression. (b,c) A small spectral region extracted from the 2D NOESY (b) and 2D ROESY (c) spectra recorded with multiple-solvent suppression. The sample is the peptide Sandostatin in H_2O and DMSO. For (a) 32 scans were recorded for each of the 400 t_1 increments and for (b,c) 16 scans were acquired for each of the 480 t_1 increments. The spectral width in both dimensions was 11.9 ppm. The data were multiplied with a cosine window function in both dimensions prior to Fourier transformation. The length of the two double-selective 180° pulses was 2.9 ms and the length of the sine-shaped gradients was 1 ms with a 200 μs recovery delay. The lengths of the WALTZ-16 sequence (Shaka et al., 1983) (a), the mixing time (b) and the spin-locking period (c) were 50, 152, 150 ms, respectively. The spin-locking condition in (c) was achieved with a train of 180deg pulses with alternating phase (Hwang and Shaka, 1992). The negative cross peaks in (b, c) have been filled for clarity. The broken line indicates the frequency of the DMSO signal.

signal is obtained. This offset difference may deviate a few Hz from the measured value in Figure 1a. The discrepancy between real and optimized solvent suppression chemical shift difference is probably due in part to the transient Bloch–Siegert effect acting during the 180° selective pulses (Emsley and Bodenhausen, 1990; Emsley, 1991). As has been shown, these effects occur also at large offsets from the carrier frequency and are more pronounced for complex pulse shapes. Furthermore, the use of a relatively strong selective 180° pulse on a solvent resonance will produce some weak resonance effects on the other solvent. In this case the approximation of adding the two pulses together is not correct anymore. As is evident from Figure 1b, the suppression of the two solvent signals after optimization is very efficient.

The suppression of the ^{13}C satellite signals of DMSO or other solvents is achieved with the application of ^{13}C selective decoupling during the ^{1}H soft 180° SLPs (Smallcombe et al., 1995). An alternative to this scheme is the use of ^{13}C hard pulses applied simultaneously with the ^{1}H hard 180° pulses. The ^{13}C satellite signals suppression is then obtained interactively by simply varying the length of these two ^{13}C hard pulses and/or the length of the gradient recovery time until minimum intensity for the ^{13}C satellite signals is reached. Application of the ^{13}C filter is shown experimentally in Figure 2. The residual ^{13}C satellite signals of DMSO present in the spectrum recorded with scheme (1) (Figure 2a) are completely suppressed in the spectrum recorded with scheme (1) with the addition of the ^{13}C filter (Figure 2b). The method described here works equally well also for systems with more solvent resonances. For example, excellent multiple solvent suppression could be achieved for compounds dissolved in 50% H_2O and 50% CH_3CH_2OH by employing SLPs with excitation at the CH_3, CH_2 and H_2O + OH frequencies, respectively (data not shown).

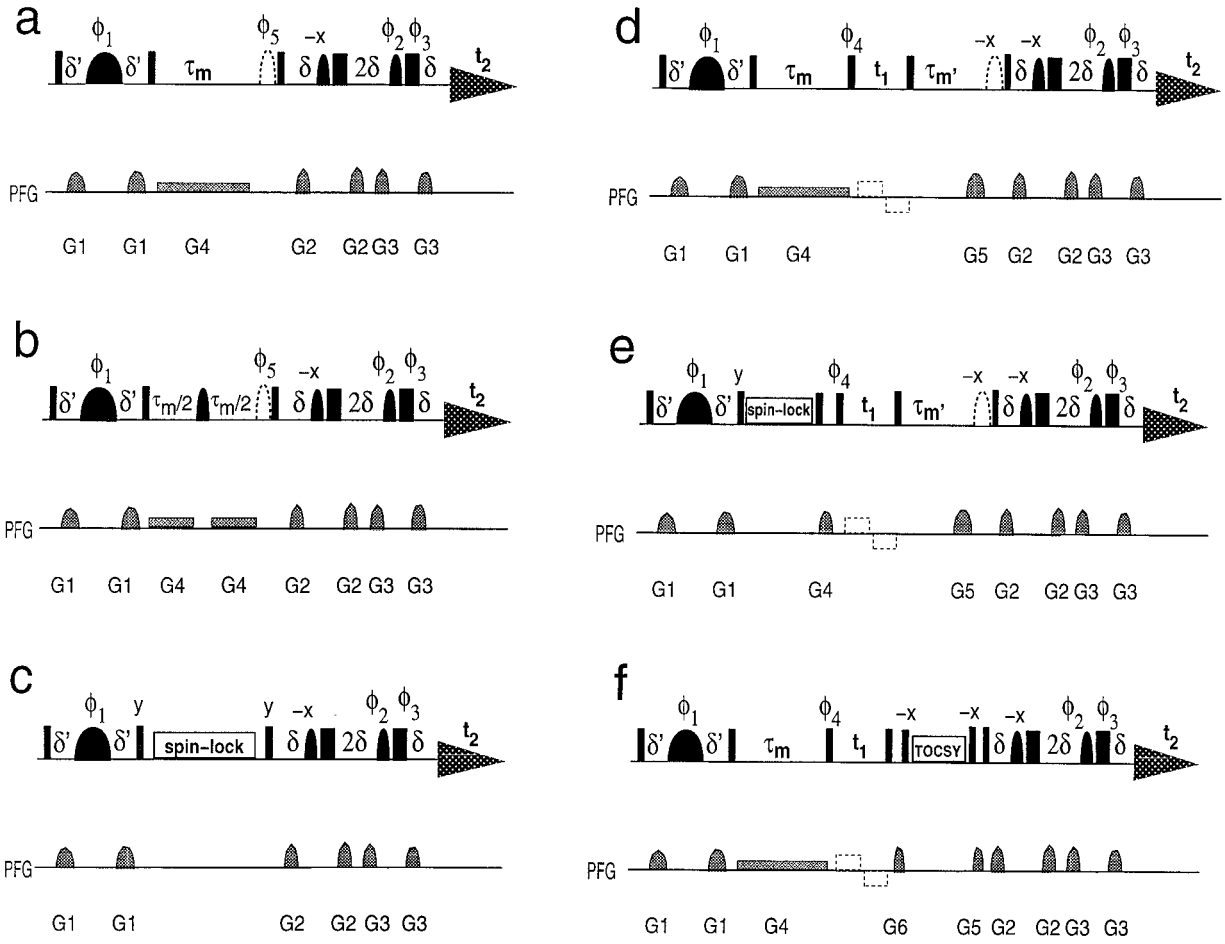

Figure 4. Pulse sequences for the homonuclear 1D ePHOGSY with NOE (a,b) and ROE (c) step and 2D ePHOGSY with NOE-NOE (d), ROE-NOE (e) and NOE-TOCSY (f) steps. The narrow and broad bars represent 90° and 180° pulses, respectively. The bipolar gradients during the evolution period (Sklenár, 1995) and the solvent flip-back 90° pulse (Grzesiek and Bax, 1993b), shown with dashed lines, are optional. The selective 180° pulse located between the first two PFGs is usually 30 to 50 ms long in order to achieve good selectivity. The two selective 180° pulses of the excitation sculpting scheme are frequency shifted laminar pulses with excitation at the solvent chemical shifts. Typically these pulses are soft rectangular pulses or strongly truncated Gaussian pulses. In the QUIET-ePHOGSY experiment (b) the selective pulse in the middle of τ_m can be a selective or semiselective 180° pulse which inverts the so-called clandestine spins. This scheme can be used also in (d) and (f). If one is interested only in the NOE between H_2O and a particular proton of the biomolecule this selective 180° pulse becomes a selective SLP applied at the H_2O and target spin frequencies. The value δ and δ' are usually equal to the length of the PFGs plus a gradient recovery time. However, δ' can contain an additional delay for filtering out the broad resonances of the protein resonating at the solvent frequency. The spin-lock in (c,e) is achieved with a continuous pulse of reduced power and phase y. The τ_m is the mixing time of the NOE step. The period $\tau_{m'}$ in (d,e) is the second mixing time. The phase cycling is important to guarantee the complete suppression of unwanted magnetization. Phases are $\phi_1 = (x, -y, -x, y)$; $\phi_2 = 4(-x), 4(y), 4(x), 4(-y)$; $\phi_3 = 4(x), 4(-y), 4(-x), 4(y)$; $\phi_4 = 16(x), 16(-x)$; $\phi_{rec} = 2(x, -x), 2(-x, x)$ in (a–c) and $\phi_{rec} = 2[2(x, -x), 2(-x, x)], 2[2(-x, x), 2(x, -x)]$ in (d–f). The two other pulses comprising the multiple-solvent suppression scheme can also be phase cycled together with the receiver with an EXORCYCLE. However, the use of only one EXORCYCLE in the multiple-solvent scheme was sufficient in our experiments to obtain excellent solvent suppression. The phase of the flip-back pulse in (a) is $\phi_5 = (-x, x)$ whereas in (b) it depends on the choice of the selective 180° pulse used for spin diffusion suppression. The phase of the other pulses is x, unless indicated otherwise. The strength and length of G1 can be varied in order to study the exchange of bound H_2O or other solvents. The gradients G2 and G3 have different strengths. These gradients should be applied in all three directions if triple-axis gradients hardware is available. This reduces the possibility of accidentally refocusing the unwanted coherence transfer pathway by the last PFG (Keeler et al., 1994). The lengths of G2 and G3 should be short in order to reduce evolution under the coupling constants. The gradient G4 in (a,d,f) is a weak rectangular PFG applied for almost the entire length of τ_m. This gradient is split in two gradients in (b) and the two PFGs can have different strength. The ^{13}C filter described in the text is also used in these schemes. Quadrature detection in ω_1 in (d–f) is achieved with the method of time-proportional phase incrementation (TPPI) (Drobny et al., 1979; Marion and Wüthrich, 1983) where the 90° pulse immediately preceding the evolution period is incremented by 90° steps in conjunction with t_1.

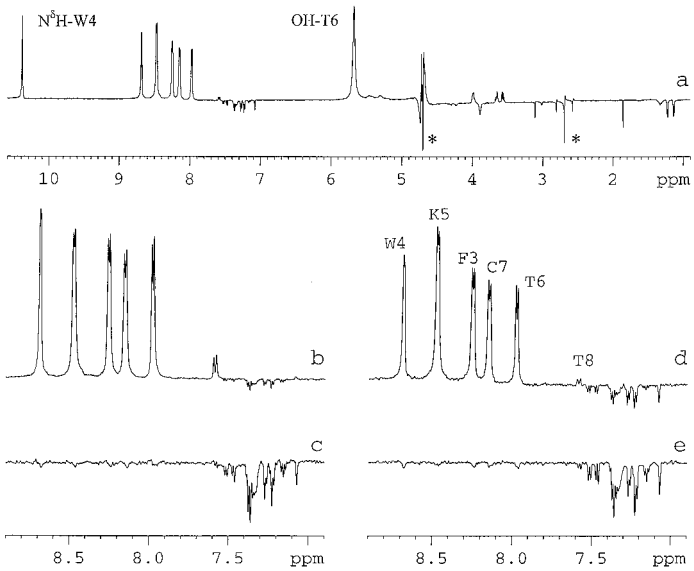

Figure 5. (a) One-dimensional ePHOGSY with ROE step recorded with the pulse sequence of Figure 4c with selective excitation at the H_2O chemical shift. (b–e) An expanded spectral region extracted from ePHOGSY-NOE (b,c) and ePHOGSY-ROE (d,e) with selective excitation at the H_2O (b,d) and DMSO (c,e) chemical shifts. The number of scans was 1024 (a), 256 (b), 4096 (c), 256 (d), 4096 (e) and no flip-back pulse was employed. The length of the first selective 180° Gaussian pulse and of the two double-selective 180° pulses was 36 and 2.9 ms, respectively. The gradient recovery delay was 200 μs and the repetition time was 2.3 s. The length of the spin-locking period was 100 ms (a,e), and 80 ms (d) and the length of the mixing time was 205 ms (b,c). Other parameters are the same as in Figure 1. The asterisks in (a) indicate the residual solvent signals. The positive peaks between 3 and 4 ppm are probably due to TOCSY transfer from the two OHs of Thr^8-Ol which resonate at the H_2O frequency. The NHs of the different amino acids are labelled.

The idea of using selective shifted laminar pulses in combination with gradients for multiple-solvent suppression was described previously (Dalvit et al., 1996) in a modified WATERGATE pulse sequence (Piotto et al., 1992). In our experience, scheme (1) achieves better multiple-solvent suppression and requires less adjustments in the optimization procedure. Another application of the SLP for multiple-solvent suppression was described in the WET pulse sequence (Smallcombe et al., 1995). It is outside the scope of this work to present a comparison of the two techniques.

It should be pointed out that Parella et al. (1998a) proposed a different pulse sequence, based also on the excitation sculpting sequence (Hwang and Shaka, 1995; Stott et al., 1995), for the suppression of multiple solvents. The selective 180° pulses are applied sequentially (Parella et al., 1998b) in this pulse sequence. For example, the suppression of two solvent signals is achieved with the use of four selective 180° pulses.

Implementation of scheme (1) in 2D TOCSY, NOESY and ROESY experiments is possible, similar to what has been done for the single solvent suppression (Callihan et al., 1996). Figure 3a shows a typical 2D TOCSY spectrum of Sandostatin and Figures 3b and 3c show a small expanded region extracted from the 2D NOESY (b) and 2D ROESY (c). The excellent multiple-solvent suppression combined with the in-phase character of the residual solvent signals allows the observation of NOEs and ROEs between the solvents and the solute. It is clear from Figures 1–3 that these experiments can be used in all NMR applications which require multiple-solvent suppression.

Insertion of scheme (1) in the 1D and 2D homonuclear ePHOGSY experiments is shown in Figure 4. The ^{13}C filter is applied as described above. The first selective 180 °C pulse in these pulse sequences is applied either at the DMSO or the H_2O frequency. Figure 5a shows a typical spectrum of a 1D ePHOGSY-ROE recorded with the pulse sequence of Figure 4c and with selective excitation applied at the H_2O chemical shift. Note the almost complete suppression of the H_2O and DMSO signals. The positive peaks correspond to chemical exchange between H_2O and exchangeable protons of the peptide, whereas the negative peaks correspond to dipolar interactions between H_2O and the peptide. The strongest exchange peak is observed for the OH resonance of Thr^6 at 5.67 ppm. This resonance was not visible in a sample of the pep-

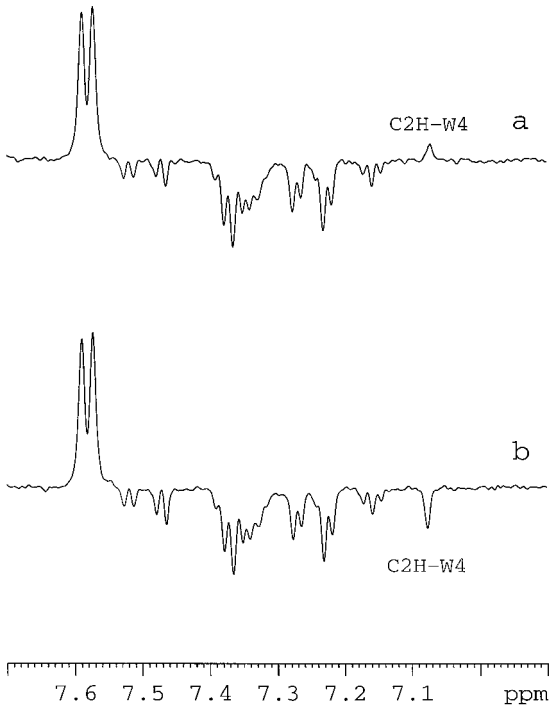

Figure 6. One-dimensional ePHOGSY-NOE recorded with selective excitation at the H_2O chemical shift (a) with the pulse sequence of Figure 4a and (b) with the pulse sequence of Figure 4b. A total of 1024 scans were recorded with a repetition time of 2.3 s and without water flip-back pulse. The length of the mixing time was 207 ms in both experiments. In (b) the selective 180° Gaussian pulse applied in the middle of the mixing time at the N^{δ}H-W4 resonance (10.38 ppm) was 4.8 ms long. Other parameters are the same as for Figure 5. The magnetization relay process $H_2O \rightarrow N^{\delta}$H-W4 $\rightarrow$ C2H-W4 is suppressed in (b) and only the direct NOE $H_2O \rightarrow$ C2H-W4 is observed.

tide diluted in 100% H_2O due to its rapid exchange with H_2O. Figures 5b–e show an expanded spectral region extracted from the 1D ePHOGSY-NOE (b,c) and 1D ePHOGSY-ROE (d,e) with selective excitation at the H_2O (b,d) and DMSO (c,e) chemical shift.

The mole fraction of DMSO in the mixture is 0.17. The viscosity of this binary solvent at 297 K is about 3 cP (Schichman and Amey, 1971), which is three times the viscosity of H_2O at the same temperature. The diffusion coefficients D of H_2O and DMSO measured with a PFG spin-echo experiment are 9.8×10^{-6} cm^2/s and 5.4×10^{-6} cm^2/s, respectively. The peptide in this viscous environment has a diffusion coefficient of 1.3×10^{-6} cm^2/s, which is similar to the D coefficient of a small protein in H_2O. For example, ubiquitin, a protein of 76 amino acids and MW 8.6 kDa, has a D of 1.5×10^{-6} cm^2/s at 298 K (Altieri et al., 1995). Therefore the peptide behaves like a large molecule ($\omega\tau_c \gg 1.1$) and the intramolecular NOEs are negative (positive cross peaks), as is seen in Figure 3b. However, as is evident from Figure 3b and Figures 5b and c, the intermolecular NOEs from both solvents to the peptide are positive (negative cross peaks), indicating a short lifetime (< 1 ns at ω^1H $= 600$ MHz) (Otting et al., 1991) of the solvent bound to the peptide. Only the NOE between H_2O and the C2H-W4 proton appears to be positive, as is shown in Figures 5b and 6a. This could represent a direct NOE from a tightly bound H_2O or a relayed NOE via the exchanging proton N^{δ}H-W4. It has been demonstrated theoretically and experimentally that indirect magnetization transfer between two spins via a third spin (*clandestine* spin) can be suppressed by selective inversion of the third spin in the middle of the mixing time (Zwahlen et al., 1994, 1996) or by a train of selective 180° selective pulses applied to the clandestine spin during the entire length of the mixing time (Fejzo et al., 1991). The scheme with a single selective 180° pulse called QUIET (Zwahlen et al., 1994) can be implemented in the ePHOGSY for the suppression of relayed magnetization. The pulse sequence of this experiment, which we call QUIET-ePHOGSY, is shown in Figure 4b. In our specific case, after the inversion of the N^{δ}H-W4 magnetization in the middle of the mixing time, the transfer of H_2O magnetization to N^{δ}H-W4 changes sign during the second half of τ_m, so that the net transfer is very small at the end of the mixing time. To first order there is no transfer of magnetization from N^{δ}H-W4 to C2H-W4 and only the direct NOE between H_2O and C2H-W4 would be observed. This is shown experimentally in Figure 6b. The experiment has been recorded with the pulse sequence of Figure 4b. The NOE to C2H-W4, which is positive in Figure 6a, becomes negative in Figure 6b demonstrating that the observation of positive NOE in Figures 5b and 6a is due to the predominant relay process $H_2O \xrightarrow{\text{exchange}} N^{\delta}$H-W4 $\xrightarrow{\text{NOE}}$ C2H-W4. Instead only the direct process $H_2O \xrightarrow{\text{NOE}}$ C2H-W4 is observed in Figure 6b. If one is interested only in the NOE between H_2O and C2H-W4, the 180° selective pulse applied in the middle of τ_m in Figure 4b is replaced with a frequency shifted laminar selective 180° pulse with excitation at the H_2O and C2H-W4 chemical shifts (Zwahlen et al., 1994). This has the effect of uncoupling the two inverted spins from all the other spins.

DMSO in the presence of H_2O appears to interact only very weakly with the NHs. It is clear that

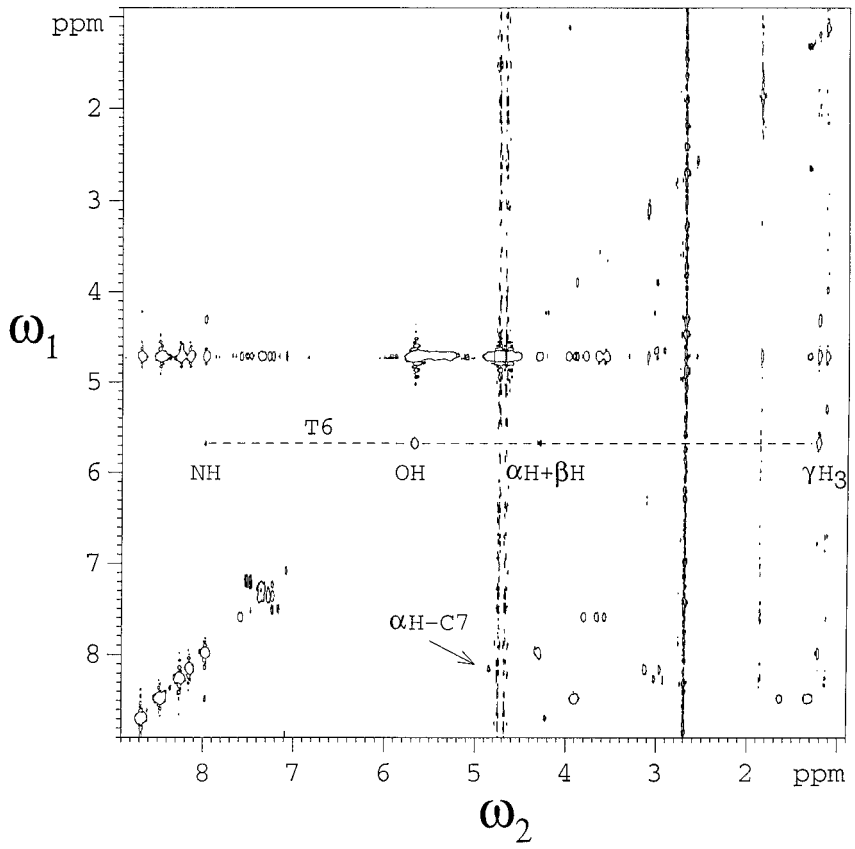

Figure 7. Two-dimensional spectrum recorded with the pulse sequence of Figure 4f for the Sandostatin sample at 297 K with selective excitation at the H_2O chemical shift. A total of 64 scans were recorded for each of the 256 t_1 increments. The repetition time, the mixing time and the TOCSY period were 2 s, 202 ms and 50 ms, respectively. The spectral width in both dimensions was 10 ppm. The data were multiplied with a cosine window function in both dimensions prior to Fourier transformation. The length of the first selective 180° Gaussian pulse and of the two double-selective 180° pulses was 36 and 2.9 ms, respectively. The gradient in the mixing time had a rectangular shape and all the other gradients had sine shape. Other parameters are the same as described in Figure 1. The two t_1 noise ridges originate from the residual solvent signals. Complete assignment for Thr^6 starting from its OH is indicated.

exchange of the NHs with H_2O will reduce in part NOEs and ROEs between DMSO and NHs. However, this mechanism cannot account for the almost complete absence of NOEs and ROEs. The NHs are well hydrated by H_2O molecules with the creation of transient intermolecular hydrogen bonds. This fact, taken together with the larger size of the DMSO molecule, could explain the limited DMSO accessibility at the NHs. However, a better comparison should be performed with NHs which do not exchange with H_2O.

For proteins, DNA- and RNA-solvent interaction studies, the 2D version of the ePHOGSY should be employed. This is necessary in order to overcome the severe problems of overlap encountered in the ^1H spectra of large biomolecules. Figure 7 shows a typical 2D ePHOGSY NOE-TOCSY spectrum recorded with the pulse sequence of Figure 4f with selective excitation applied at the H_2O chemical shift. The two t_1 noise ridges represent the residual solvent signals. The baseline in these spectra is flat due to the pure-phase character of the residual solvent signals. Therefore, as evident in Figure 7, the limit in signal detection is solely dependent on the thermal noise and the small t_1 noise originating from the diagonal peaks. Three different types of signals are observed in these spectra: (i) The signals at $\omega_1 = \omega H_2O$ originate from H_2O magnetization transfer during the spin-locking period after the evolution period t_1. These are the same signals observed in the 2D TOCSY, NOESY or ROESY experiments of Figure 3. (ii) The signals on the diagonal originate from H_2O magnetization transfer during the period τ_m before t_1. (iii) The cross peaks originate from H_2O magnetization transfer during τ_m

and homonuclear Hartmann–Hahn transfer during the spin-locking period. Assignment for the spin system of Thr^6 starting from the OH resonance is shown. The use of the selective 180° pulses does not allow the observation of the peaks which resonate in ω_2 close to the solvent signals. However, this bleached spectral region is not large. In our experience the use of soft square 180° SLPs of length between 2.8 and 6 ms allows good selectivity. The cross peak corresponding to the H^{α} resonance of Cys^7, which is at only 0.14 ppm from H_2O, although attenuated, is clearly visible in Figure 7. For proteins the pulse sequence of Figure 4d should be used in order to reduce signal losses due to fast T_2 relaxation.

In conclusion, we have shown that a simple modification of the excitation sculpting sequence in combination with an optimization procedure results in 1D and 2D spectra with excellent multiple-solvent suppression. Its implementation in the ePHOGSY experiments allows the observation and identification of the interactions of organic solvents or small molecules with biological macromolecules. Finally, it has been shown that the QUIET-ePHOGSY experiment permits the differentiation of direct and relayed NOEs between H_2O and a particular proton of the protein.

Acknowledgements

The author thanks Prof. L. Emsley for helpful discussions concerning the selective pulses and Dr. T. Parella for stimulating discussions and for personal communication.

References

Altieri, A.S., Hinton, D.P. and Byrd, R.A. (1995) *J. Am. Chem. Soc.*, **117**, 7566–7567.
Bauer, C., Freeman, R., Frenkiel, T., Keeler, J. and Shaka, A.J. (1984) *J. Magn. Reson.*, **58**, 442–457.
Birlirakis, N., Cerdan, R. and Guittet, E. (1996) *J. Biomol. NMR*, **8**, 487–491.
Böckmann, A. and Guittet, E. (1996) *J. Biomol. NMR*, **8**, 87–92.
Bodenhausen, G., Freeman, R. and Turner, D.L. (1977) *J. Magn. Reson.*, **27**, 511–514.
Callihan, D., West, J., Kumar, S., Schweitzer, B.I. and Logan, T.M. (1996) *J. Magn. Reson.*, **B112**, 82–85 (1996).
Clore, G.M., Bax, A., Wingfield, P.T. and Gronenborn, A.M. (1990) *Biochemistry*, **29**, 5671–5676.
Dalvit, C. and Hommel, U. (1995) *J. Magn. Reson.*, **B109**, 334–338.
Dalvit, C. (1996) *J. Magn. Reson.*, **B112**, 282–288.
Dalvit, C., Ko, S.Y. and Böhlen, J.M. (1996) *J. Magn. Reson.*, **B110**, 124–131.
Drobny, G., Pines, A., Sinton, S., Weitekamp, D.P. and Wemmer, D. (1979) *Symp. Faraday Soc.*, **13**, 49.
Emsley, L. and Bodenhausen, G. (1990) *Chem. Phys. Lett.*, **168**, 297.
Emsley, L. (1991) Ph.D. Thesis, University of Lausanne, Lausanne.
Fejzo, J., Westler, W.M., Macura, S. and Markley, J.L. (1991) *J. Magn. Reson.*, **92**, 195–202.
Grzesiek, S. and Bax, A. (1993a) *J. Biomol. NMR*, **3**, 627–638.
Grzesiek, S. and Bax, A. (1993b) *J. Am. Chem. Soc.*, **115**, 12593–12594.
Hwang, T.-L. and Shaka, A.J. (1992) *J. Am. Chem. Soc.*, **114**, 3157–3158.
Hwang, T.-L. and Shaka, A.J. (1995) *J. Magn. Reson.*, **A112**, 275–279.
Hwang, T.-L., Mori, S., Shaka, A.J. and Van Zijl, P.C.M. (1997) *J. Am. Chem. Soc.*, **119**, 6203–6204.
Keeler, J., Clowes, R.T., Davis, A.L. and Laue, E.D. (1994) *Methods Enzymol.*, **239**, 145–207.
Kriwacki, R.W., Hill, R.B., Flanagan, J.M., Caradonna, J.P. and Prestegard, J.H. (1993) *J. Am. Chem. Soc.*, **115**, 8907–8911.
Liepinsh, E. and Otting G. (1997) *Nat. Biotechnol.*, **15**, 264–268.
Marion, D. and Wüthrich, K. (1983) *Biochem. Biophys. Res. Commun.*, **113**, 967–974.
Moonen, C.T.W., Van Gelderen, P., Vuister, G.W. and Van Zijl, P.C.M. (1992) *J. Magn. Reson.*, **97**, 419–425.
Mori, S., Johnson, M.O., Berg, J.M. and Van Zijl P.C.M. (1994) *J. Am. Chem. Soc.*, **116**, 11982–11984.
Mori, S., Berg, J.M. and Van Zijl, P.C.M. (1996) *J. Biomol. NMR*, **7**, 77–82.
Otting, G. and Wüthrich, K. (1989) *J. Am. Chem. Soc.*, **111**, 1871–1875.
Otting, G. Liepinsh, E. and Wüthrich, K. (1991) *Science*, **254**, 974–980.
Otting, G. and Liepinsh, E. (1995*) J. Biomol. NMR*, **5**, 420–426.
Parella, T., Adell, P., Sanchez-Ferrando, F. and Virgili, A. (1998a) *Magn. Reson. Chem.*, in press.
Parella, T., Sanchez-Ferrando, F. and Virgili, A. (1998b) *J. Magn. Reson.*, in press.
Patt, S.L. (1992) *J. Magn. Reson.*, **96**, 94–102.
Piotto, M., Saudek, V. and Sklenár, V. (1992) *J. Biomol. NMR*, **2**, 661–665.
Ponstingl, H. and Otting, G. (1997) *J. Biomol. NMR*, **9**, 441–444.
Schichman, S.A. and Amey, R.L. (1971) *J. Phys. Chem.*, **75**, 98–102.
Shaka, A.J., Keeler, J. and Freeman, R. (1983) *J. Magn. Reson.*, **53**, 313–340.
Shuker, S.B., Hajduk, P.J., Meadows, R.P. and Fesik, S.W. (1996) *Science*, **274**, 1531–1534.
Sklenár, V. (1995) *J. Magn. Reson.*, **A114**, 132–135.
Smallcombe, S.H., Patt, S.L. and Keifer, P.A. (1995) *J. Magn. Reson.*, **A117**, 295–303.
Stott, K., Stonehouse, J., Keeler, J., Hwang, T.-L. and Shaka, A.J. (1995) *J. Am. Chem. Soc.*, **117**, 4199–4200.
Wider, G., Riek, R. and Wüthrich, K. (1996) *J. Am. Chem. Soc.*, **118**, 11629–11634.
Zwahlen, C., Vincent, S.J.F., Di Bari, L., Levitt, M.H. and Bodenhausen, G. (1994) *J. Am. Chem. Soc.*, **116**, 362–368.
Zwahlen, C., Vincent, S.J.F., Schwager, M. and Bodenhausen, G. (1996) *Chem. Eur. J.*, **2**, 45–49.